Mechanism for performance of energetically modified cement versus corresponding blended cement

Harald Justnes[a,*], Lennart Elfgren[b], Vladimir Ronin[b]

[a]*SINTEF Civil and Environmental Engineering, Cement and Concrete, N-7465 Trondheim, Norway*
[b]*Luleå University of Technology, Sweden*

Abstract

The microstructure of cement paste of 50/50 mixes of cement/quartz and cement/fly ash, both ground in a special mill [energetically modified cement (EMC) process] and simply blended, have been studied under sealed curing conditions. The grinding process reduced the size of both cement grains and quartz/fly ash markedly and created flaky agglomerates of high inner surface for the finer particles. EMCs had much higher degree of hydration at 1 day, but similar as blends at 28 days. The pores were much finer for EMC paste due to smaller particles as also reflected in the strength. The morphology of calcium hydroxide in EMC paste appeared more mass like. Pozzolanic reaction was insignificant for quartz in EMC, but increased for fly ash. Thus, improved performance of EMC versus OPC can be explained by increased early hydration and extensive pore size refinement of the hardened binder resulting in reduced permeability and diffusivity for concrete.

1. Introduction

Energetically modified cement (EMC) is produced by high intensive grinding/activation of ordinary Portland cement (OPC) together with different types of fillers. The EMC process was developed at Luleå University of Technology and at EMC Development from 1994. Some properties of EMC with 50% filler may be comparable to, and even better than, OPC. Studies on the performance of EMC have been published by Ronin et al. [1–3], Jonasson et al. [4], Rao et al. [5], Groth and Ronin [6], Hedlund et al. [7], and Johansson et al. [8].

A project characterizing concrete with EMC as compared to OPC was carried out by SINTEF a few years back [9]. The paper is focusing on mechanisms to explain the performance of EMC versus OPC as summarized by Sellevold [9].

2. Experimental

2.1. Materials

Four cementitious powders were made by EMC Development, Luleå, Sweden. These powders were denoted

- EQ = 50/50 standard Portland cement from Slite, Sweden/quartz sand ground in a vibrating mill according to the EMC-technology.
- Q = a simple blend (not milled) of the same components as in EQ.
- EFA = 50/50 standard Portland cement from Slite, Sweden/Class F fly ash from Danash, Denmark, ground in a vibrating mill according to the EMC-technology.
- FA = a simple blend (not milled) of the same components as in EFA.

The chemical composition of cement and fly ash is summarized in Table 1.

The mechanical modification of the preceding blends was carried out in a Humboldt Palla 20 U vibrating mill. The charge of 2 kg material was subjected to 30 min

* Corresponding author. Tel.: +47-73596922; fax: +47-73597136.
E-mail address: harald.justnes@sintef.no (H. Justnes).

Table 1
Composition of cement, quartz filler, and fly ash

Compound	OPC	Quartz filler	Fly ash
CaO	65.7	2.2	2.5
SiO_2	19.7	73.9	53.0
Al_2O_3	5.5	13.1	25.0
Fe_2O_3	2.8	2.6	9.5
SO_3	2.6	3.4	–
Na_2O	0.1	3.9	–
K_2O	1.6	<0.02	–

Table 2
Specific surfaces, S (m^2/kg), and solids densities, ρ_s (kg/m^3), of powders

Powder	EQ	Q	EFA	FA
S_{psd}	270	134	330	261
S_{bet}	2210	710	3790	1600
S_{bla}	566.2	259.5	693.5	452.0
ρ_s	2910	2900	2830	2700

milling with 10 mm diameter and 150 rpm vibrating cycle.

Pastes were made by mixing EQ and Q with distilled water to w/s = 0.40 and EFA and FA to w/s = 0.5 (because they had higher water demand); w/s means in this case water-to-solid ratio by mass. The pastes were filled on glass vials with plastic lids. Q paste had a high tendency of separation (FA only marginal), thus the vials of these were rotated perpendicular to their axes until the paste had set. The EQ and EFA pastes were not rotated because they were stable towards segregation.

The first terminus for stopping of hydration should be close to the moment of setting. This was done by quenching the samples in liquid nitrogen (−196 °C) every half hour from 4 h and thawing them in 96% ethanol. When the sample retained its shape, instead of falling apart to a powder, this time was taken as the first terminus. It was about 6 h for EQ and EFA and 12 h for Q and FA. The objective was to stop all at about the same low degree of hydration so pore size distribution could be a measure of different particle packing from the very beginning. After 4 h on replenished ethanol to remove free water, the samples were dried at 105 °C for 16 h to remove physical bound water.

All paste samples were in addition stopped at the termini 1, 3, 7, and 28 days by crushing the vials (note the sealed curing conditions at 20 °C), breaking the sample into small bits and storing them on excess 96% ethanol (replenished

twice) for 4–5 h before they were dried at 105 °C for 16 h to remove the evaporable water.

2.2. Characterization

The particle size distributions of the four powders were characterized by a Coulter counter (i.e., laser granulometry) after 1 min in ultrasound with water as the dispersing liquid. The particle size distribution is calculated assuming spherical particle shapes and the outer surface of the particles can be calculated under this assumption.

The specific surface of the powders was measured by nitrogen adsorption according to BET, which can be taken as a total surface (outer and inner). In addition, the powders were characterized by the standardized Blaine method. As a necessary input for the latter method, the average particle density of all the powders were measured using helium pychnometry (HeP).

The dry powders were stirred into epoxy resin that was cut and plane polished after hardening. In addition, lumps of hardened paste were impregnated with the same epoxy resin under vacuum, and cut and plane polished after the epoxy resin had hardened. The samples were coated with a carbon layer in vacuum to conduct electrons before subjected to scanning electron microscopy (SEM) investigations.

The samples for differential thermal analysis/thermo gravimetry (DTA/TG) were crushed to a fine powder and dried at 105 °C (i.e., to remove physically adsorbed water). The DTA/TG experiments were carried out at a NETZSCH 409 STA with a heating rate of 10 °C/min until 1000 °C and nitrogen as a carrier gas. The sample (≈ 150 mg) was contained in an alumina crucible and alumina powder was used as a reference. The accuracy of the temperature determined for phase transitions was within ± 2 °C, while the accuracy of the mass losses was within ± 0.3 mg. Data from the first terminus (6 or 12 h curing) was recorded on a Toledo apparatus with sample masses in the range 550–900 mg to enhance signal/noise.

The samples for mercury intrusion porosimetry/helium pychnometry (MIP/HeP) were bits of about 5 mm size. The
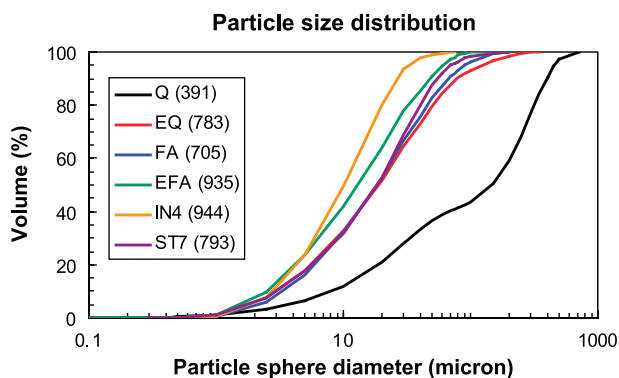

Fig. 1. Particle size distributions of EQ, Q, EFA, and FA compared to the Norwegian Portland cements ST7 and IN4. Values in parentheses after the legends are calculated surfaces of assumed spherical particles in meter squared per liter.

Table 3
Calculated initial volume fractions (vol.%) of the constituents in pastes

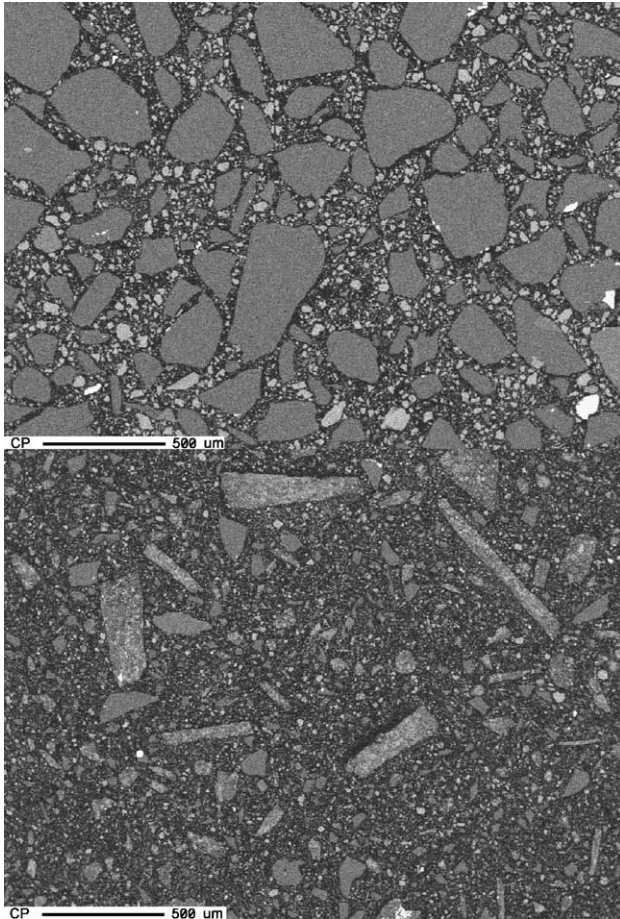| Paste	Water	Cement	Filler
EQ/Q, w/s = 0.40	53	21	26
FA, w/s = 0.50	57	19	24
EFA, w/s = 0.50	58	19	23

Fig. 2. BEIs (× 40) of powders Q (upper) and EQ (lower) embedded in epoxy resin. The large, evenly gray grains in the upper image are quartz, while the lighter gray particles are cement grains. The bright white grains often embedded in the quartz grains (in minority) are contaminations of the quartz sand taken from the mining industry (i.e., various heavy metal sulphides and barium sulphate). In the lower image (EQ), it is quite clear that the milling process has effectively ground both the quartz and the cement. However, the vibrating mill with some shear forces has also produced some flaky (looks more like rods because it is a cross-section) agglomerates of the finer cement and quartz grains.

MIP experiments were carried out with the Carlo Erba Porosimeter (Model 2000) that records the pore size (radii) distribution of the sample between 50 and 500,000 Å, assuming cylindrical pores. The density of solid material, ρ_s, was determined by Micrometrics AccuPyc 1330 He-pycnometer, while the particle density, ρ_p, was determined by Carlo Erba Macropores Unit 120. The accuracy of total porosity is within ± 0.5 units and the density within ± 0.01 units.

3. Results and discussion

3.1. Dry powders

The milling process had a considerable influence on particle size distribution and fineness. The particle size distributions are plotted in Fig. 1 and compared to a Norwegian standard Portland cement (ST7) and a finely ground rapid cement (IN4). The values in parentheses after the legends are the ''outer'' surface in meter squared per liter of the particles calculated assuming spherical particles only. This calculated outer surface is divided by the particle density and denoted S_{psd} (m^2/kg) in Table 2 where it is compared to the total (outer and inner) surface from BET, S_{bet}, and the outer surface from Blaine measurements, S_{bla}. The average densities of the particles in the powders are also given in Table 2 as obtained from HeP.

The ratio $S_{bet}/S_{psd} = 8.2$, 5.3, 11.5, and 6.1 for the powders EQ, Q, EFA, and FA, respectively, while the ratio $S_{bet}/S_{bla} = 3.90$, 2.74, 5.47, and 3.54 for the same powders. This indicates that the inner surface has increased more than the outer surface in the milling process, which can be subscribed to an increased number of cracks, etc., in the particles.

Note that the particle size distributions of EQ and EFA in Fig. 1 are close to the one for the Norwegian standard Portland cement (ST7) and coarser than for the Norwegian rapid Portland cement (IN4).

The measured average density of solids are about the same for EQ and Q, but significantly higher for EFA as compared to FA. The latter is probably due to crushing of hollow spheres in the grinding process that otherwise may be inaccessible to helium. If the density of cement is taken as 3.15 kg/m^3, the density of quartz, fly ash, and ground fly ash can be calculated to 2.65, 2.25, and 2.50 kg/m^3, respectively. The volume fractions of the constituents can then be calculated and are presented in Table 3. The volume fraction of water represents the initial porosity. Despite the different w/s, the values in Table 3 are not all that different for EQ/Q and EFA/FA.

The backscattered electron images (BEIs) from SEM of dry EQ and Q powders stirred into epoxy resin are compared at × 40 magnification in Fig. 2. Evidently, the milling process is highly efficient. It can be seen that quartz and cement are ground and agglomerates of mixed fines of quartz and cement are formed, both on a larger scale as flakes (appearing as several 100-μm rods in the cross-section) and

Table 4
Concentration of ions (g/l and [mmol]) in water from fresh paste as a function of time

Sample	K^+	Na^+	OH^-	SO_4^{2-}	Σ
EQ 10 min	10.0 [256]	1.08 [47]	1.27 [75]	–	–
EQ 1 h	10.6 [271]	1.13 [49]	2.60 [153]	8.61 [90]	[− 12]
EQ 2 h	10.2 [261]	0.99 [43]	1.96 [115]	–	–
Q 10 min	11.8 [302]	1.40 [61]	1.83 [108]	12.6 [131]	[− 7]
Q 1 h	12.0 [307]	1.42 [62]	2.26 [133]	11.8 [123]	[− 10]
Q 2 h	12.0 [307]	1.42 [62]	2.53 [149]	11.1 [116]	[− 11]
EFA 10 min	7.87 [201]	0.90 [39]	1.80 [106]	6.98 [73]	[− 11]
EFA 1 h	8.30 [212]	0.93 [41]	2.15 [126]	6.89 [72]	[− 17]
EFA 2 h	7.85 [201]	0.90 [39]	2.22 [131]	6.48 [67]	[− 26]
FA 10 min	9.39 [240]	1.16 [50]	1.52 [89]	–	–
FA 1 h	9.73 [249]	1.20 [52]	2.02 [119]	9.41 [98]	[− 14]
FA 2 h	9.67 [247]	1.20 [52]	2.40 [141]	8.82 [92]	[− 25]

The weighted sum of charges, Σ (mmol), is calculated as well.

Table 5
Features from thermal analysis for EQ paste as a function of time

Age	Tot (%)	α (%)	CH (%)	CH/Tot (%)
6 h	5.08	41	2.21	43
1 day	8.88	71	8.10	91
3 days	8.63	69	10.21	118
7 days	8.89	71	10.31	116
28 days	9.48	76	10.58	112

Table 7
Features from thermal analysis for EFA paste as a function of time

Age	Tot (%)	α (%)	CH (%)	CH/Tot (%)
6 h	6.89	28	4.11	60
1 day	8.64	69	8.65	100
3 days	9.93	79	9.28	93
7 days	10.38	83	9.18	88
28 days	11.15	89	7.37	66

even as small grains of the size of ordinary cement grains. If these smaller agglomerates are not broken up by the ultrasound prior to the particle size distribution measurements, they will appear as rather coarse grains, but the inner surface will be high. This explains the difference between the specific surfaces S_{psd} and S_{bet} (see Table 2).

Note that the paste samples here were made by hand mixing without any dispersing admixtures (i.e., plasticizers). It is thus believed that in practical concrete technology, both the physiochemical action of plasticizers (if used) and the mechanical action of coarse aggregate will diminish the presence of at least the coarser EMC agglomerates. Higher magnification SEM inside a large agglomerate in EQ reveals that it consists of particles from 10 μm down to a submicron level. Quartz particles of 1 μm and below might be reactive towards alkaline water when mixed with cement over time, in particular if the milling is so powerful that strains are induced in the lattice of quartz.

The BEIs from SEM of dry EFA and FA powders stirred into epoxy resin reveals that the milling process also in this case formed flaky agglomerates in EFA, appearing as long rods in the cross-section image. No agglomerates are visible in FA. The fly ash particles appear either as hollow spheres or porous, layered particles consisting essentials of Al and Si as detected by energy dispersive spectra (EDS).

3.2. Hydrated cement pastes and mortars

3.2.1. General observations from paste mixing

The Q blend was mixed first with w/s = 0.40 and the mix was very unstable (large separation tendencies). Thus, the glass vials with samples were rotated perpendicular to their axes until setting to obtain uniform hardened pastes. When EQ was mixed with the same w/s, the paste was very sticky and hard to blend.

When the FA was tried to be mixed with w/s = 0.40, it turned out too dry and additional water was added to w/s = 0.50. There was then only a weak tendency of separa-

tion, but still the sample vials were rotated to ensure uniform hardened paste samples. The EFA mixed with w/s = 0.50 showed no sign of separation, but was still easy to blend. However, the color of this mix was much darker than FA and there was a sootlike layer floating on top. This is an indication of crushed fly ash spheres exposing insufficiently burnt material to the water phase.

3.2.2. Ions in the water phase of fresh paste

The water phase of the paste mixes described in Section 3.2.1 was filtered off on a Büchner funnel using vacuum from a water pump after 10 min, and 1 and 2 h. At first, the concentration of K^+, Na^+, and OH^- were measured. Because the charge balance then showed high concentration of unidentified anions, the sulphate concentration was determined as well. However, a few samples had not enough water left to perform this latter analysis. The results are given in Table 4.

Note that the ion concentrations in EFA/FA systems are lower than in EQ/Q systems due to the higher w/s. As a control, the sulphate concentrations and hydroxyl concentration after 10 min for FA was multiplied with 5/4, giving the exact values as measured for Q.

The hydroxyl concentration rapidly reaches a concentration corresponding to a pH slightly in excess of 13 for all samples, even for EFA/FA with higher w/s.

The high sulphate concentration comes from the easily soluble alkali sulphates in the clinker, because the solubility of the calcium sulphates added during the milling of the clinker are sparingly soluble. Calcium sulphate results in sulphate concentrations in the range 14–21 mmol, depending on the amount of crystal water. A Portland cement has a sulphate content typically corresponding to 3.5% SO_3, while the clinker itself may have $1 \pm 0.5\%$ SO_3. Assuming the present cement to have easily soluble alkali sulphates corresponding to 1% SO_3, this would give a sulphate concentration in the water phase of Q of 15 g/l, which is not too

Table 6
Features from thermal analysis for Q paste as a function of time

Age	Tot (%)	α (%)	CH (%)	CH/Tot (%)
12 h	5.57	44	4.00	72
1 day	5.63	45	4.81	85
3 days	7.09	57	7.85	111
7 days	8.37	67	9.67	115
28 days	9.49	76	11.05	116

Table 8
Features from thermal analysis for FA paste as a function of time

Age	Tot (%)	α (%)	CH (%)	CH/Tot (%)
12 h	7.30	29	3.90	53
1 day	7.96	64	6.92	87
3 days	9.73	78	8.67	89
7 days	10.20	82	8.62	85
28 days	10.89	87	8.25	76

Table 9
Compressive strength ± standard deviation (MPa) of standard mortars (EN197) at different termini after water curing

Powder	EQ	Q	EQ·100%/Q (%)	EFA	FA	EFA·100%/FA (%)
1 day	10.4 ± 0.4	1.8 ± 0.2	578	13.3 ± 0.7	5.1 ± 0.3	261
3 days	18.3 ± 0.7	4.5 ± 0.3	407	21.5 ± 0.8	13.4 ± 0.7	160
7 days	21.8 ± 0.7	5.7 ± 0.3	382	24.6 ± 0.6	14.8 ± 0.9	166
28 days	32.7 ± 1.2	8.4 ± 0.4	389	41.2 ± 1.6	26.6 ± 0.7	155

Six prism end pieces were tested for each strength.

far from the initial measured value of 12.6 g/l. The initial value declines over time as the sulphate combine with reacting C_3A to ettringite. The sulphate level is smaller for the milled compared to the blended samples due to their higher surface and hence more exposed C_3A.

The ions analyzed give a nearly complete composition of the water phase, but there is a small concentration of undefined anions corresponding to a residual negative charge in the range 1–5%.

3.2.3. Thermal analyses of paste

Four features of the pastes were extracted from the DTA/TG curves at the different termini: Tot = total mass loss from 105 to 1000 °C in percentage of the ignited powder = total chemical bound water. α = Degree of hydration for the 50% cement fraction assuming that 25% water is chemically bound in a completely hydrated cement. CH = the content of calcium hydroxide in percentage of the ignited powder. CH/Tot = the ratio between calcium hydroxide and total chemical bound water content in percent. The results are given for EQ, Q, EFA, and FA in Tables 5–8, respectively.

It is probably only meaningful to calculate the degree of hydration for EQ and Q based on the chemical bound water, at least at higher ages, because the pozzolanic reaction of fly ash also will lead to a change in, probably more, chemically bound water. The EQ paste reached 71% hydration already at 1 day, and was thereafter rather constant with only a marginal increase between 7 and 28 days to 76%. The hydration of the cement in Q is more gradual because it is much coarser, but the hydration of Q and EQ is equal at 28 days. The content of calcium hydroxide relative to the total chemical bound water increases for both EQ and Q until 3 days, then flattens out on a rather equal level. The only exception is a marginal decrease for EQ at 28 days that could indicate a minor pozzolanic activity between CH and

very small or strained quartz grains. The CH content in EQ and Q of about 11% corresponds to 22% in the cement paste, which is in line with the expected level (about 25% for a fully hydrated cement).

For the EFA and FA pastes, the total mass loss is only marginally higher for EFA than for FA at different termini. The CH content reaches a higher level in EFA than in FA at 1 day, but decreases faster as a function of time and reaches a lower level at 28 days. This indicates that the pozzolanic reaction of fly ash is faster in EFA (already between 1 and 3 days) than in FA (mostly between 7 and 28 days), which is understandable considering that spherical shells in the fly ash are crushed in the milling process, allowing simultaneous reaction on two sides of the glassy fly ash wall.

3.2.4. Compressive strength of mortars

One test for functional improvement of cement blends by the milling process is compressive strength development versus time. The compressive strengths of standard (EN197) mortars based on EQ, Q, EFA, and FA powders are reproduced in Table 9 for different termini of water curing.

There is a substantial strength increase for mortars with milled cements (EQ and EFA) compared to their blended analogues (Q and FA). The difference is larger at 1 day and seems to be on a relative constant level from 3 days on persisting until at least 28 days. The average mass of EQ, Q, EFA, and FA prisms were 586 ± 2, 583 ± 2, 578 ± 2, and 575 ± 2 g, respectively. The relative values indicates that the huge difference at 1 day is mostly due to increased hydration, while the rather constant level from 3 to 28 days is an effect of finer particles and pores in the binder.

It is pointed out in Table 3 that the phase volumes in the different pastes are not all that different in spite of different w/s. Thus, the much higher strength level of FA mortar versus Q mortar (Table 9) is difficult to understand. How-

Table 10
Specific surface (S_g), particle density (ρ_p), solid density (ρ_s), mercury accessible porosity (ε_{Hg}), and helium accessible porosity (ε_{He}) of EQ pastes as a function of curing time

Age	S_g (m²/g)	ρ_p (kg/m³)	ρ_s (kg/m³)	ε_{Hg} (vol.%)	ε_{He} (vol.%)
6 h	11.58	1370	2720	45.8	49.6
1 day	18.37	1475	2387	37.4	38.2
3 days	20.57	1492	2323	34.5	35.8
7 days	23.69	1456	2297	34.0	36.6
28 days	24.13	1487	2268	33.5	34.4

Table 11
Specific surface (S_g), particle density (ρ_p), solid density (ρ_s), mercury accessible porosity (ε_{Hg}), and helium accessible porosity (ε_{He}) of Q pastes as a function of curing time

Age	S_g (m²/g)	ρ_p (kg/m³)	ρ_s (kg/m³)	ε_{Hg} (vol.%)	ε_{He} (vol.%)
12 h	7.22	1441	2676	44.8	46.1
1 day	8.91	1472	2599	40.4	43.4
3 days	10.67	1450	2490	38.3	41.8
7 days	13.14	1538	2431	35.1	36.7
28 days	14.52	1571	2358	33.5	33.4

Table 12
Specific surface (S_g), particle density (ρ_p), solid density (ρ_s), mercury accessible porosity (ε_{Hg}), and helium accessible porosity (ε_{He}) of EFA pastes as a function of curing time

Age	S_g (m²/g)	ρ_p (kg/m³)	ρ_s (kg/m³)	ε_{Hg} (vol.%)	ε_{He} (vol.%)
6 h	8.35	1300	2588	48.2	49.8
1 day	19.97	1302	2373	43.7	45.2
3 days	32.76	1349	2264	39.3	40.4
7 days	30.61	1377	2235	37.6	38.4
28 days	40.20	1349	1931	31.7	30.1

ever, the chemical bound water for FA paste (Table 8) is much higher than for Q paste (Table 6) until 7 days. At 28 days, there is, in addition, significant pozzolanic reaction in the FA mix. Due to the finer particles, the pore sizes in the FA mix will be much smaller than in the Q mix. However, it cannot be ruled out that the strength of mortar with unstable Q paste is unusually low due to partial separation or internal flaws.

The somewhat higher compressive strength of EFA mortar compared to the EQ mortar is associated with the somewhat higher chemical bound water in Table 7 versus Table 5 (except for 1 day) and finer particles (i.e., higher surface in Table 2). The larger difference at 28 days is attributed to additional pozzolanic activity of fly ash not found for the quartz at 20 °C sealed curing.

3.2.5. Porosity and pore size distribution of hydrated paste

The specific surface (S_g), particle density (ρ_p), solid density (ρ_s), mercury accessible porosity (ε_{Hg}), and helium accessible porosity (ε_{He}) of the pastes as a function of curing time have been measured by a combination of MIP and HeP. The surface tension of mercury was taken as 480 dyn/cm, the contact angle 140° and cylindrical shaped pores was assumed. The results for EQ, Q, EFA, and FA pastes are given in Tables 10–13, respectively. The pore size distribution for all pastes cured at 6–12 h and 1, 3, 7, and 28 days are plotted in Figs. 3–7, respectively.

The general usual trends are that the porosity decreases as a function of time and the specific surface increases as a function of time as the pores become smaller in size but higher in numbers (e.g., gel pores). The porosity of the milled species is smaller than the blended analogues at any age until at least 7 days due to higher degree of hydration,

Table 13
Specific surface (S_g), particle density (ρ_p), solid density (ρ_s), mercury accessible porosity (ε_{Hg}), and helium accessible porosity (ε_{He}) of FA pastes as a function of curing time

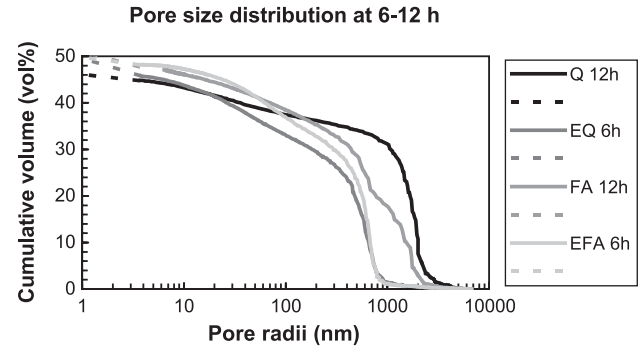| Age	S_g (m²/g)	ρ_p (kg/m³)	ρ_s (kg/m³)	ε_{Hg} (vol.%)	ε_{He} (vol.%)
12 h	9.68	1231	2519	47.7	51.1
1 day	15.53	1243	2359	44.7	47.3
3 days	22.72	1313	2260	38.4	41.9
7 days	20.70	1383	2248	35.9	38.5
28 days	27.15	1371	2102	34.7	34.8

Fig. 3. Pore size distribution of EQ (w/s = 0.40) and EFA (w/s = 0.50) pastes cured for 6 h at 20 °C and Q (w/s = 0.40) and FA (w/s = 0.50) pastes cured for 12 h at 20 °C. Solid line from MIP and dashes line residual porosity from HeP.

but is rather equal at 28 days (as the chemical bound water and w/s are equal). The average density of solids decreases as a function of time due to increasing amount of crystal water as hydration proceeds.

The pore radii at half the porosity for every paste is extracted from Figs. 3–7 and listed in Table 14. It shows clearly the pore refinement by decreasing pore size as a function of time. However, note that despite the equal porosity at, for instance, 7 days curing, the pore size at half porosity is much smaller for the milled species (EQ and EFA) than for the blended species (Q and FA). This is attributed to decreased grain size and improved particle packing already at the casting stage.

The similar total porosity of EFA and FA compared to EQ and Q, despite the higher w/s of 0.50 versus 0.40, is understandable from the calculated volume fractions in Table 3. After all, the initial porosity (at theoretical time zero) is 53% for EQ/Q, 57% for FA, and 58% for EFA, which is reasonable compared to the helium accessible porosity immediately after set of 49.6 (6 h), 46.1 (12 h), 49.8 (6 h), and 51.1 % (12 h) for EQ, Q, EFA, and FA pastes, respectively.

The porosity of EQ after 28 days with $\alpha = 0.76$ (i.e., degree of hydration) can be calculated assuming w/c = 0.80 (w/s = 0.40, 50% c). The amount of chemical bound water
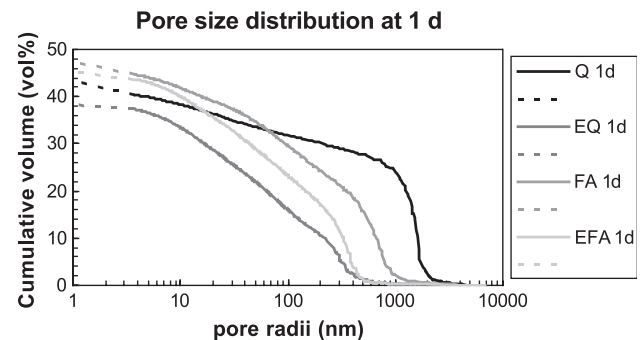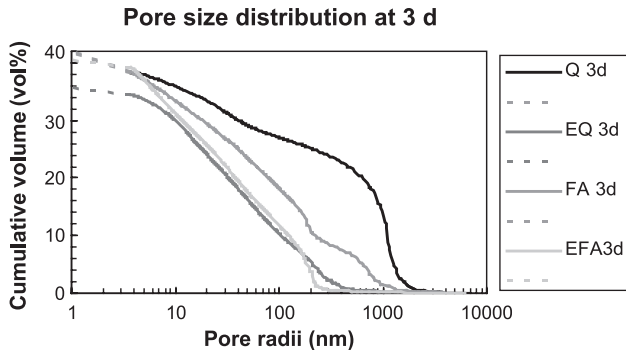

Fig. 4. Pore size distribution of EQ and Q (w/s = 0.40) and EFA and FA (w/s = 0.50) pastes cured for 1 day at 20 °C. Solid line from MIP and dashes line residual porosity from HeP.

Pore size distribution at 3 d

Fig. 5. Pore size distribution of EQ and Q (w/s = 0.40) and EFA and FA (w/s = 0.50) pastes cured for 3 days at 20 °C. Solid line from MIP and dashes line residual porosity from HeP.

Pore size distributions at 28 days

Fig. 7. Pore size distribution of EQ and Q (w/s = 0.40) and EFA and FA (w/s = 0.50) pastes cured for 28 days at 20 °C. Solid line from MIP and dashes line residual porosity from HeP.

will be $0.25 \cdot \alpha = 0.190$, while the amount of physical absorbed water in the CSH gel (i.e., in gel pores) will be $0.15 \cdot \alpha = 0.114$ (evaporates at 105 °C). Because the hydration products has a lower volume than cement and water, there will be formed contraction pores corresponding to $0.25 \cdot 0.25 \cdot \alpha = 0.048$. Thus, there will be a certain volume of evaporable water at 105 °C corresponding to $(w/c) - 0.25 \cdot \alpha = 0.610$. The total porosity, ε_t (including gel pores) of this hardened cement paste will then be $(0.048 + 0.610) \cdot 100\% / \rho_w \cdot (1/\rho_c + (w/c)/\rho_w) = 65.8\% / 1.117 = 58.9$ vol.%. This must be multiplied with the volume fraction 0.747 (see Table 3) of paste to give the porosity of EQ or Q paste to 44.0 vol.%. The measured helium accessible porosity for EQ and Q paste with 76% degree of hydration is 34.4 and 33.4 vol.%, respectively, which means that only 3/4 of the total estimated porosity is accessible to both mercury and helium.

If one excludes the very fine gel porosity of CSH and only estimates capillary and contraction pores; $((w/c) - 0.4 \cdot \alpha + 0.25 \cdot 0.25 \cdot \alpha) \cdot 100\% / \rho_w \cdot (1/\rho_c + (w/c)/\rho_w)$ one obtains 40.1% for the cement paste fraction and 30.0% for the EQ or Q paste. This corresponds very well with the observed porosity considering the crude estimates and that may be some of the coarser gel pores may be accessible. One can thus state that, in
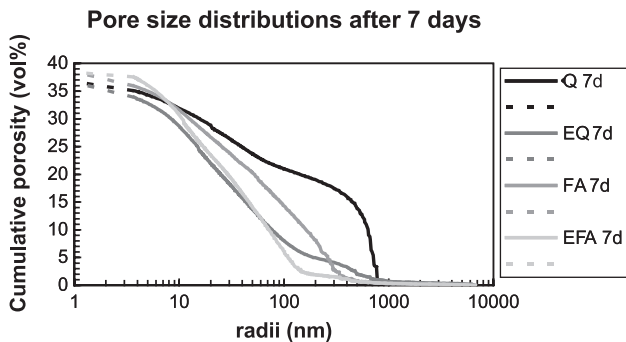
general, the capillary pores and contraction pores from chemical shrinkage will dominate the porosity observed by Hg intrusion porosimetry and He pycnometry.

3.2.6. SEM investigation of hydrated pastes

The general trends observed for the EQ an Q pastes are the following:

- There are still agglomerates in the EQ paste that are not completely dispersed (no plasticizers was used), but to a much lesser extent than in the powder itself.
- CH crystals prefer quartz as a substrate for growth.
- There is little sign of pozzolanic reaction between calcium hydroxide and quartz within the 28 days of sealed curing.
- Q paste has much coarser, regular CH crystals as compared to the more mass-like CH morphology in EQ often embedding small quartz grains (example in Fig. 8).
- Porosity is much higher in Q than in EQ pastes (see 1 day example in Fig. 8).
- Q paste at 12 h had significant amounts of syngenite that did not appear in EQ at 6 h, probably due to the higher surface with larger amount of exposed C_3A consuming the sulphate. Syngenite has formula $K_2Ca(SO_4)_2 \cdot 2H_2O$ [or $K\bar{C}\bar{S}_2 \cdot 2H$ by cement chemist's short hand] and crystallises as tablets or prisms. It occurs in the early stage of cementitious systems as a reaction between potassium sulphate and gypsum (especially for cements high in potassium).

Pore size distributions after 7 days

Fig. 6. Pore size distribution of EQ and Q (w/s = 0.40) and EFA and FA (w/s = 0.50) pastes cured for 7 days at 20 °C. Solid line from MIP and dashes line residual porosity from HeP.
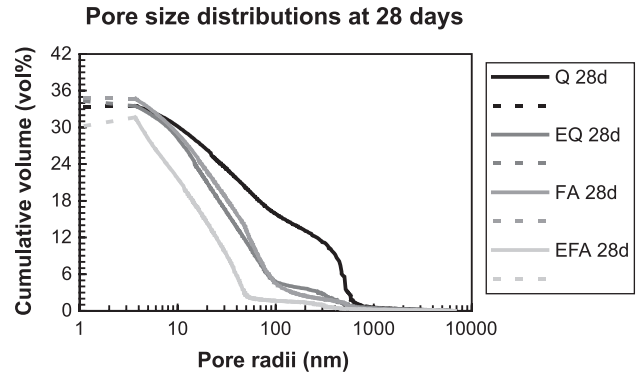
Table 14
Pore radii (nm) at 50% of total volume intruded by Hg for different pastes as a function of curing time

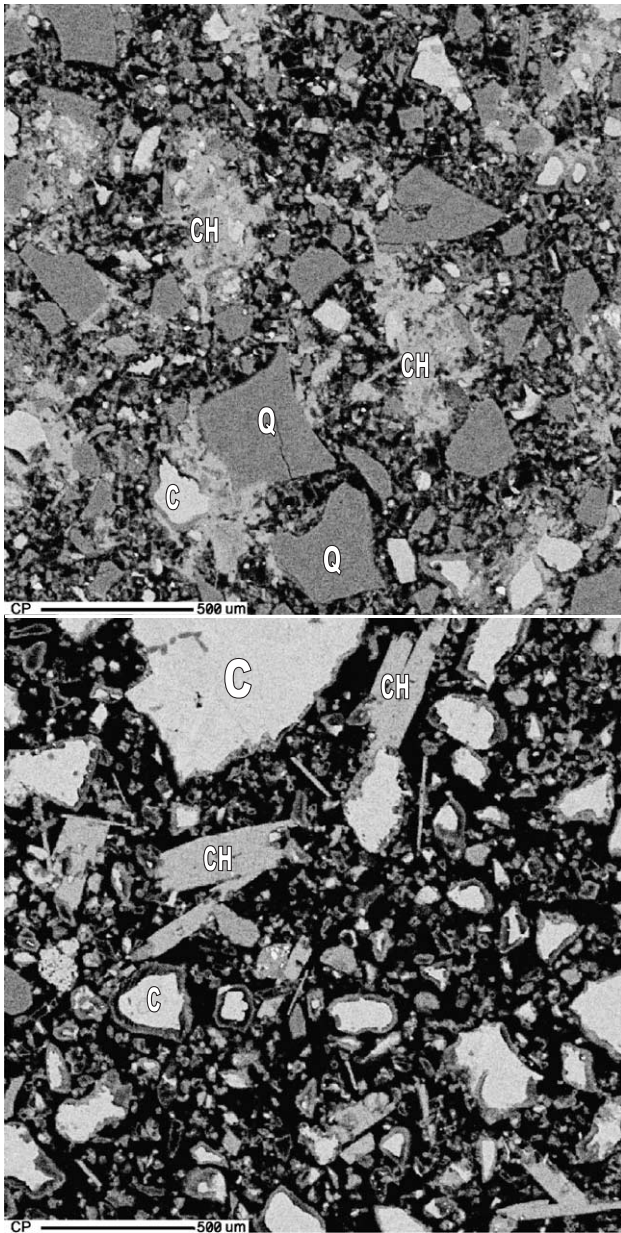| Paste/age	Q	EQ	FA	EFA
6 h		435		478
12 h	1574		638	
1 day	1254	74	259	119
3 days	710	45	88	39
7 days	298	35	65	33
28 days	82	30	35	18

Fig. 8. BEIs (× 500) of EQ (upper) and Q (lower) cured for 1 day. Calcium hydroxide regions are marked with CH in both cases. The CH in EQ has an irregular, cloudy nature often embedding finer particles, while CH in Q appears as large platy crystals. Note also that the binder appears much more porous (black area = pores) in Q than in EQ. This can be some of the reasons for the difference in CH morphology, because CH crystals are given space to grow in the Q paste. Note also the more open reaction rims (CSH) around the cement grains in Q versus EQ. Cement grains marked "C" and quartz grains marked "Q".

The general observations of hydrated EFA/FA pastes by SEM are about the same as for EQ/Q pastes above, with the exception of the latter point about syngenite. In addition, CH crystals in the FA paste are less coarse than for the Q paste. A comparison of EFA and FA paste after 7 days curing is reproduced in Fig. 9.

4. Conclusions

The following conclusions can be drawn on the mechanism of improved performance of EMC versus OPC from the study of 50/50 mixes of cement/quartz and cement/fly ash both ground in a special mill and simply blended.

The grinding process reduces the size of both cement grains and quartz/fly ash extensively and creates agglomerates of essentially flaky nature for the finer particles. This
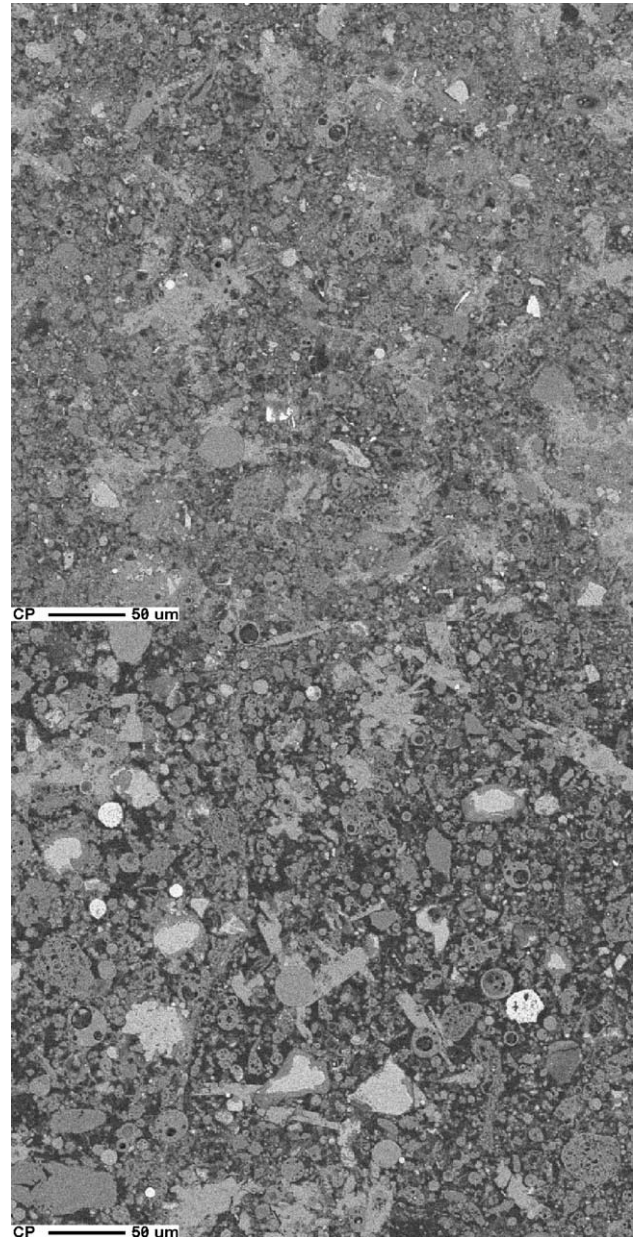

Fig. 9. BEIs (× 250) of EFA and FA pastes cured for 7 days at 20 °C. The matrix of FA is more porous than the matrix of the EFA paste, and there are more unreacted cement grains in the FA paste. The light gray areas of calcium hydroxide seems to be mass like in EFA paste, and a mix of mass-like and larger individual crystals in the FA paste (probably a matter of available space).

gives a particle size distribution of the ground powders comparable to OPC and rapid cement, but with specific surface $\approx$ 3 times higher as measured by N_2 adsorption.

The ground cement has a very high degree of hydration at 1 day that flattens out at sealed conditions. The blend reaches about the same degree of hydration at 28 days and similar total porosity. However, the pores are much finer for paste based on the ground powders. Capillary and contraction pores dominate measured porosity, while the gel pores of the CSH are essentially inaccessible to Hg and He.

Differences in degree of hydration and pore refinement are reflected in the compressive strength of mortars based on the same powders. The increase in relative compressive strength is very high at 1 day and than the difference continues to rise at a much smaller rate until 28 days (last terminus tested).

The morphology of calcium hydroxide in paste based on the milled powders is more mass like, often embedding fine particles of, for instance, quartz, making them an integral part of the binder. Calcium hydroxide in paste based on the blended powders appears as larger single crystals probably due to the available space for growth in a matrix with coarser pores. This difference may also contribute to the improved performance of the ground powder (EMC) versus OPC/filler blends.

Calcium hydroxide seems to prefer quartz as a substrate for crystal growth. Within the investigated 28 days of sealed curing, there was no sign of significant pozzolanic reaction between calcium hydroxide and quartz. The milling process improved the pozzolanic activity of the fly ash and evidence of crushed spheres was seen (e.g., increased solid density of powder, darker color, and soot on the surface of fresh paste).

In short, improved performance of EMC (intensively milled 50/50 cement/powder) versus OPC/filler blends can be explained by increased early hydration and better distribution of hydration products resulting in an extensive pore size refinement of the hardened binder. The pore size refinement will lead to reduced permeability and diffusivity, which has been demonstrated in a variety of water and chloride transport properties in EMC concrete [9].

References

[1] V. Ronin, J.-E. Jonasson, Investigation of the effective winter concreting with the usage of energetically modified cement (EMC)—material science aspects, Report, vol. 1994:03, Div. of Struct. Eng., Luleå Univ. of Techn., Luleå, Sweden, 1994, 24 pp.

[2] V. Ronin, J.-E. Jonasson, High strength and high performance concrete with use of EMC hardening at cold climate conditions, in: K. Sakai, N. Banthia, O.E. Gjørv (Eds.), Proceedings of the International Conference on Concrete under Severe Conditions, vol. 2, E.&F.N. Spon (ISBN 0419 19860 2), Sapporo, Japan, 1995 (August, 2–4), pp. 898–906.

[3] V. Ronin, J.-E. Jonasson, H. Hedlund, Advanced modification technologies of the Portland cement based binders for different high performance applications, in: H. Justnes (Ed.), Proceedings of the 10th International Congress on the Chemistry of Cement, vol. 2ii077, Inform Trycket AB (ISBN 91-630-5496-5), Gothenburg, 1997 (June 2–6), 8 pp.

[4] J.-E. Jonasson, V. Ronin, H. Hedlund, High strength concretes with energetically modified cement and modeling of shrinkage caused by self-desiccation, in: F. de Larrard, R. Lacroix (Eds.), Proceedings of the 4th International Symposium on the Utilization of High Strength/High Performance Concrete, vol. 2, Presses Pont et Chaussees (ISBN 2-85978-258-3), Paris, France, 1996 (May 29–31), pp. 245–254.

[5] K.H. Rao, V. Ronin, K.S.E. Forssberg, High performance energetically modified Portland blast-furnace cements, in: H. Justnes (Ed.), Proceedings of the 10th International Congress of the Chemistry of Cement, vol. 3ii104, Inform Trycket AB (ISBN 91-630-5497-5), Gothenburg, 1997 (June 2–6), 9 pp.

[6] P. Groth, V. Ronin, Influence of energetically modified cement on interfacial bond and fracture toughness in cement-based fiber reinforced composites, in: I. Holand, E.J. Sellevold (Eds.), Proceedings of the 5th International Symposium on Utilization of High Strength/High Performance Concrete, Norwegian Concrete Association, Oslo, 1999 (ISBN 82-91341-25-7), Sandefjord, 1999 (June 20–24), pp. 1114–1123.

[7] H. Hedlund, V. Ronin, J.-E. Jonasson, Ecological effective high performance cement based binders, in: I. Holand, E.J. Sellevold (Eds.), Proceedings of the 5th International Symposium on Utilization of High Strength/High Performance Concrete, Norwegian Concrete Association, Oslo, 1999 (ISBN 82-91341-25-7), Sandefjord, 1999 (June 20–24), pp. 1144–1153.

[8] K. Johansson, C. Larsson, O.N. Antzutkin, W. Forsling, K.H. Rao, V. Ronin, Kinetics of the hydration reactions in the cement paste with mechanochemically modified cement ^{29}Si magic-angle-spinning NMR study, Cem. Concr. Res. 29 (1999) 1575–1581.

[9] E.J. Sellevold: Summary and evaluation of SINTEF test results on energetically modified cements (EMC), SINTEF Report STF22 F98764, 1998-09-18, 8 pp. Issued by SINTEF, Trondheim, Norway.